ELSEVIER

Marine Geology 183 (2002) 17–29

MARINE GEOLOGY
INTERNATIONAL JOURNAL OF MARINE GEOLOGY, GEOCHEMISTRY AND GEOPHYSICS

www.elsevier.com/locate/margeo

Role of wave groups in resuspension of sandy sediments

J.J. Williams [a,*], C.P. Rose [b], P.D. Thorne [a]

[a] *Proudman Oceanographic Laboratory, Bidston Observatory, Bidston Hill, Prenton CH43 7RA, UK*
[b] *Tessella Support Services PLC, 3 Vineyard Chambers, Abingdon OX14 3PX, UK*

Received 30 November 2000; accepted 7 September 2001

Abstract

Field measurements of the resuspension of medium/coarse sand by orthogonal wave–currents in approximately 20 m water depth are presented and discussed. Velocity squared-suspended sediment cospectra indicate resuspension events occur at incident wave frequencies $O(12\ s)$ and at lower frequencies $O(60\ s)$ corresponding approximately to wave groups. Wave run-length parameters, determined for six wave records, are used to quantify bottom sediment response to wave group forcing. Results show that under groups of more than five waves, average suspended sediment concentration values, C, are approximately three times larger than values measured beneath a single wave of comparable height. Analyses demonstrate that the apparent in situ grain settling velocity also increases under groups of waves. A simple empirical expression, which quantifies the wave group influence on the near-bed 'reference' suspended sediment concentration, is presented.

Keywords: wave group; enhanced sediment concentration; sediment resuspension

1. Introduction

In marine situations, waves are characterised by temporal scales ranging from individual waves to groups of waves. In the case of wave groups, the short-wave time-average momentum flux, or radiation stress, and the mass flux vary relatively slowly through time. Temporal and spatial variation in radiation stress and mass flux generates long waves with periods and wavelengths similar to the wave group period and length (Longuet-Higgins and Stewart, 1964). In physical terms, a wave group containing larger than average waves depresses the water surface and thereby forces a long wave. At offshore locations, these long waves may travel with the group, or may be released if the wave groups forcing them change rapidly, for example through shoaling or through breaking. Long waves released at the coast may be trapped by refraction as edge waves, or may escape to deep water.

Whilst attention has been drawn to the importance of wave groups in the resuspension of sea bed sediments (e.g. Hanes and Huntley, 1986; Mase, 1989; Hanes, 1991; Sato, 1992; Lee et al., 1994; Bedford and Lee, 1994), few studies have attempted to address the question of how wave grouping affects the near-bed suspended sediment concentration, C, and the vertical C profile (e.g. Jimenez et al., 2000). Here, field measurements of suspended sediments and waves obtained during a storm from a location adjacent to Mid-

* Corresponding author.
E-mail address: jjw@pol.ac.uk (J.J. Williams).

0025-3227/02/$ – see front matter
PII: S0025-3227(01)00251-1

delkerke Bank are used to investigate wave group effects upon sediment resuspension (Fig. 1a). This large offshore sand bank in the southern North Sea, Europe, has been studied extensively in two projects examining the geological history (RESECUSED, De Moor et al., 1993), and the present day dynamics of offshore sand banks (CSTAB, O'Connor, 1996).

2. Experimental description

The present data were obtained at the northern end of Middelkerke Bank in the Flemish Banks at 51°20.6′N 02°46.3′E, shown in Fig. 1a. Surficial sediments comprise graded medium/coarse sand (measured median grain diameter, $D_{50} = 450$ μm and still water median terminal settling velocity, $w_{s50} = 6.2$ cm/s, Fig. 1b). Observed bottom morphological features included sandwaves with wavelength, λ, ≈ 200 m and height, h, ≈ 3 m and mega-ripples (λ, ≈ 15 m and h, ≈ 1 m). Further details of the field site are given by (O'Connor, 1996).

Data used in the following sections relating to surface waves, tidal currents and vertical suspended sediment concentration profiles were obtained in approximately 20 m water depth using a suit of sensors on the autonomous multi-sensor instrument STABLE (Sediment Transport And Boundary Layer Equipment, Humphery and Moores, 1994), Fig. 1c. Measurements of water depth at wind wave frequencies were obtained using a Digiquartz pressure sensor, PS, at height z above the sea bed ≈ 170 cm. Valeport Series 800 electromagnetic current meters, ECMs, were used to measure the orthogonal flow components U, V and W at $z \approx 40$ cm and 80 cm. Here, U and V denote flow in the horizontal plane and W denotes flow in the vertical plane. ECM sensors had a diameter of 10 cm and a sensitivity of ± 0.1 cm/s. ECM sensors were arranged at 90° to each other and separated horizontally by 20 cm. Measurements of the concentration of suspended sediments were obtained approximately 15 cm in front of the ECM sensors at vertical intervals of 1 cm from the bed up to $z \approx 128$ cm using dual frequency acoustic backscatter sensors, ABS, operating at 1.0 MHz and 2.5 MHz (Thorne et al., 1993). Data from the PS and from the ECMs were sampled at 8 Hz and were logged at hourly intervals in burst mode for a period spanning approximately 19 min. Synchronous data from the ABS system were sampled at 4 Hz and were logged in burst mode for a period spanning approximately 17 min.

The present paper considers six observational periods (bursts 34–burst 39) spanning approximately 6 h during a moderate storm. Waves and currents were approximately orthogonal and significant wave height during this period, H_s, fell in the range 2.1–2.9 m, depth-mean tidal currents exceeded 70 cm/s and burst-averaged suspended sediment concentrations, $\bar{C}_b$ at $z = 2$ cm were of the order of 0.03 g/l. Instantaneous suspended sediment concentration exceeded 10 g/l close to the bed. Surface waves observed during this period where characterised by a well-developed groupy structure.

3. Data analysis

3.1. Hydrodynamic parameters

Data from the ECMs were calibrated, screened for noise spikes and corrected for sensor misalignment in the vertical plane ($\approx 5°$), for sensor zero drift (at worst < 1 cm/s during the observational period considered here) and for zero-offset errors using the methods described by Soulsby et al. (1991) and Hannay et al. (1994). Data from adjacent ECM heads were then combined to obtain the instantaneous values for the horizontal flow components U and V using

$$U = \hat{U}_s \cos(45°) + \hat{U}_p \sin(45°) \quad (1)$$

$$V = \hat{U}_s \sin(45°) - \hat{U}_p \cos(45°) \quad (2)$$

where $\hat{U}$ is the measured instantaneous horizontal flow velocity from either the starboard, s, or port, p, ECM head in the pair (Fig. 1c). The zero-mean horizontal flow components u and v comprising turbulence and wave motion were calculated from $u = U - \bar{U}$ and $v = V - \bar{V}$, respectively, where

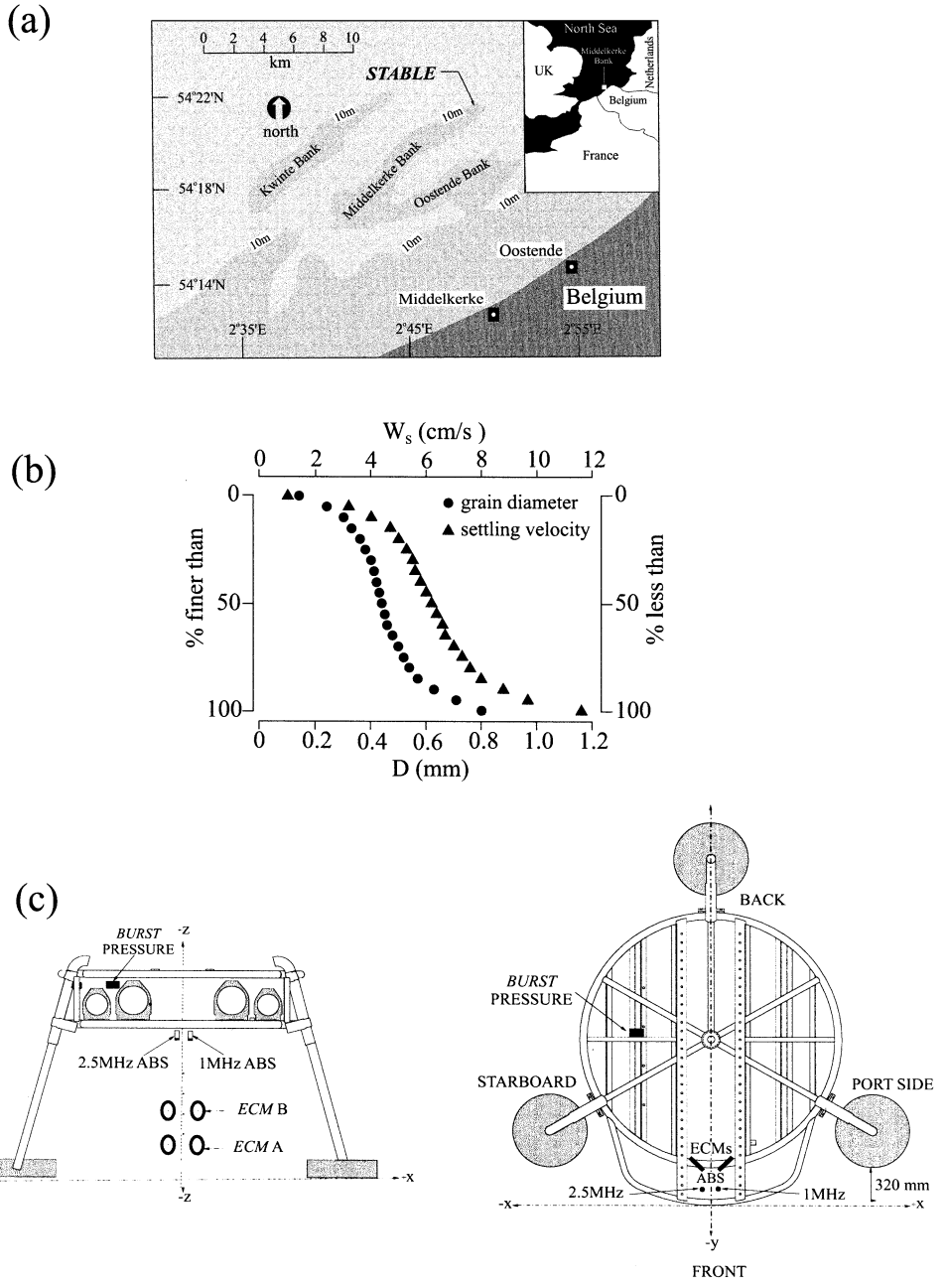

Fig. 1. (a) Location of the field site, Middelkerke Bank, Flemish Banks, southern North Sea, Europe. (b) Cumulative grain size and terminal grain settling velocity for surficial sediment at the field site. (c) The STABLE (Sediment Transport And Boundary Layer Equipment) frame showing principal sensors for waves, tides and suspended sediments.

$\bar{U}$ and $\bar{V}$ are the time-average values of the U and V time-series. Further details of the methodologies used here to correct ECM data are given by Hannay et al. (1994).

Time-series of water surface elevation were obtained by applying a laboratory-derived calibration to PS data. In order to obtain time-series of surface waves used in subsequent analyses of wave groups, linear wave theory was used to correct for the frequency-dependent, depth-attenuation of wave-induced bottom pressure (Bishop and Donelan, 1987; Southgate and Oliver, 1989) and a refining correction was used to account for tidal current effects (Hedges, 1978). Whilst in this water depth surface elevation values derived by this method are subject to limitations imposed by the accuracy linear of wave theory, values for H_s and peak wave period, T_P, measured by an adjacent waverider wave buoy was found to agree to within 5% of values for H_s and T_P derived from the pressure record (Williams et al., 2000).

3.2. Wave groups

Many concepts to describe wave grouping have been proposed in the literature including; statistics of run-lengths (Goda, 1985); wave grouping from analysis of water surface elevation (List, 1991); correlogram; phase spectrum; and concepts based upon the hydrodynamics of wave motion (Mansard and Sand, 1994). In a study of wave groups by Lee et al. (1994), it was concluded that wave run-length statistics best parameterise wave group enhancement of sediment resuspension. In the present study, a modified form of the Goda (1985) run-length method was used.

Using zero down-crossing analysis, individual waves occurring in wave records for burst 34 to burst 39 during the storm were identified. The first wave in a wave group is defined as being one whose amplitude is greater than a defined threshold value, H_T. In the present study, a value for H_T was defined as being the average of the smallest 20% of waves in burst 34 (i.e. 40 cm). If they are larger than their predecessor, consecutive waves following this first wave are included in the group until the maximum wave amplitude in a group is reached. As wave height decreases from the maximum value, successive waves continue to be included in the group providing their amplitude is less than the preceding wave and is greater than H_T. Allowance is also made for single waves in a given group which either fail to exceed the threshold criterion, are smaller than the preceding wave in an ascending sequence of waves, or are larger than the preceding wave in a descending sequence of waves. In such circumstances, these waves are included in the group providing that the next wave in the sequence meets the criterion stated above. This allowance for waves not conforming to the normal group pattern is found necessary if groups comprising only small numbers of waves are to be avoided.

The Goda wave group run-length, j_1, is defined as the number of waves in a wave group identified by the method above and the temporal separation between groups, j_2, is defined as the number of waves between successive wave groups. A third wave group parameter found particularly useful in the context of the present study is given the symbol j_3 and is defined as the number of waves in a group proceeding and including the largest wave. A pictorial definition of the terms j_1, j_2, j_3 and H_T is given in Fig. 2. Fig. 2 also defines the average, $\bar{a}_G$ and peak, $\hat{a}_G$, wave group amplitude, zero down-crossing wave period, T_0, and wave height, H. Investigations were also undertaken to ascertain the effect on group statistics if the value of the threshold parameter H_T was changed. It was found that providing H_T values were in a range from 40 cm to a value approximately 30% less than H_s, group statistics remained the same.

With the start and end time of each wave and wave group in a given time-series record now defined (Fig. 2), the peak wave orbital velocity, $\hat{U}_{mGroup}$, for the largest wave in each group ($\hat{a}_G$) was then estimated from the ECM data at $z \approx 40$ cm using

$$\hat{U}_{mGroup} = (\hat{U}_G^2 + \hat{V}_G^2)^{0.5} \quad (3)$$

where $\hat{U}_G$ and $\hat{V}_G$ are the peak values of U and V at the same instance in time. Estimates of the peak wave-only bed shear velocity for a given group, $\hat{U}_{*mGroup}$, was then calculated from

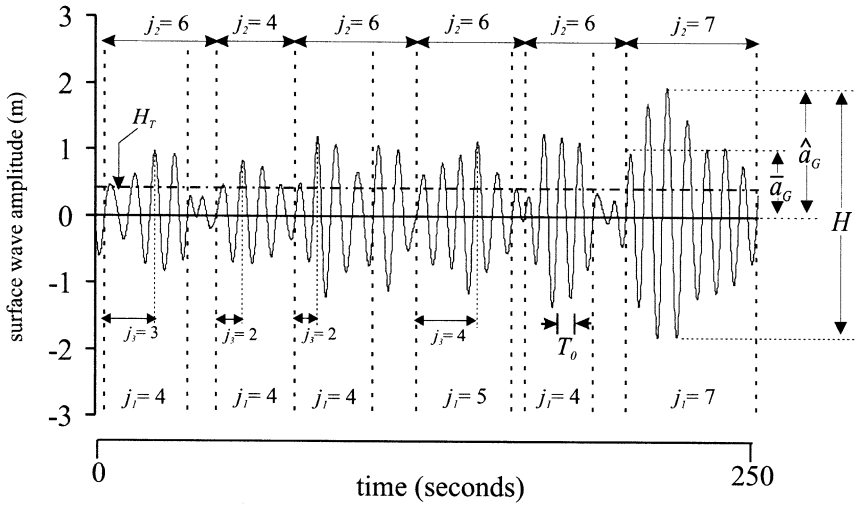

Fig. 2. Identification of wave groups in burst 36 using the Goda method showing the definition of the terms H_T, T_o, H, $\bar{a}_G$ and $\hat{a}_G$ and values for the parameters j_1, j_2 and j_3.

$$\hat{U}_{*\mathrm{wGroup}} = (0.5 f_w \hat{U}^2_{\mathrm{mGroup}})^{1/2} \quad (4)$$

where f_w is a wave friction factor. In the present study f_w was calculated using

$$f_w = \exp\left[-6 + 5.2\left(\frac{\hat{A}}{k_s}\right)^{-0.19}\right] \quad (5)$$

where $\hat{A}$ is the peak semi-orbital wave excursion given by $(\hat{U}_{\mathrm{mGroup}} T/2\pi)$, T is the period of the largest wave in a given group and k_s is a physical bed roughness parameter, (Jonsson, 1966). Bedforms were not measured, and thus estimates of the bed roughness, k_s were calculated from $8h^2/\lambda$ (Nielsen, 1992), where h and λ are the predicted height and wavelength, respectively, of vortex ripples on the sea bed. Burst-averaged values for h and λ were estimated using the using empirical formula derived by Nielsen (1981) for irregular waves which relates a sediment mobility number, Ψ_s, to h and λ using

$$\frac{\lambda}{\bar{A}} = 2.2 - 0.345\,\Psi_s^{0.34} \text{ for } 2 < \Psi_s < 230 \quad (6a)$$

$$\frac{h}{\bar{A}} = 21\,\Psi_s^{-1.85} \text{ for } \Psi_s > 10 \quad (6b)$$

where $\Psi_s = (\bar{A}\omega)^2/(\{\rho_s - \rho/\rho\})gD_{50}$, the burst-averaged semi-orbital wave excursion $\bar{A} = \bar{U}_b T_p/2\pi$, $\bar{U}_b$ is the burst-averaged wave orbital velocity calculated from the ECM data, T_p is the peak surface elevation obtained from the burst pressure spectrum, $\omega = 2\pi/T_p$, ρ is the density of sea water (1.027 g/cm^3 at 7°C), ρ_s = measured sediment density (2.65 g/cm^3), and g is the acceleration due to gravity. Here, the value of T_p derived from the pressure record was very similar to the peak wave period recorded by the adjacent waverider buoy. Further discussion of bed ripples and k_s values observed and calculated for the study period considered here is given by Williams et al. (1999).

3.3. Suspended sediments

ABS instruments were calibrated in the laboratory using in situ samples of surficial sediments obtained from the experimental site (Wylie et al., 1994; Thorne and Hardcastle, 1997). ABS time-series measurements at various heights above the sea bed were then used to calculate statistical properties of the measured suspended sediment concentration pertaining during the passage of a given wave or group of waves. Parameters used in the present study include: the average suspended sediment concentration beneath individual waves

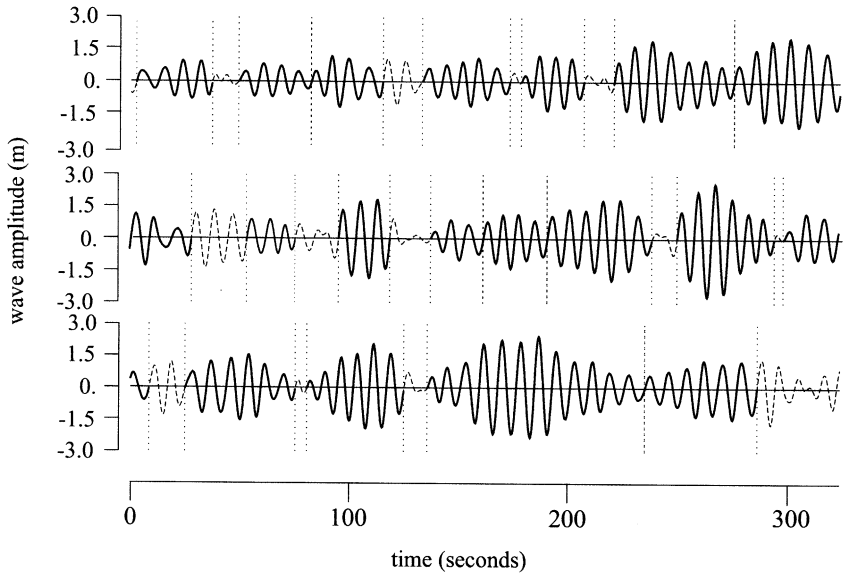

Fig. 3. Time-series plot showing surface waves and wave groups identified using a modified form of the Goda wave run-length method for burst 36.

at height z, $\bar{C}_w(z)$; the average suspended sediment concentration under a given wave group at a given height above the bed, $\bar{C}(z)$; and the peak suspended sediment concentration under a given wave group at a given height above the bed, $\hat{C}(z)$.

4. Results and discussion

Fig. 3 shows a time-series record of surface wave amplitude for burst 36 spanning a period of approximately 16 min. The well-developed groupy nature of the wave record is shown clearly. Groups of waves (solid line) are separated by waves (dashed line) failing the various groupiness criterion. The groupiness characteristics of bursts 34, 35, 37, 38 and 39 were similar to those for burst 36.

Time-series plots of j_1, $\hat{U}_{mGroup}$, $\hat{C}(z)$ and $\bar{C}(z)$ at $z = 2$ cm for bursts 34–39 are shown in Fig. 4. For all bursts, j_1 values fall in the range 2–10 and fluctuate in an apparently random fashion

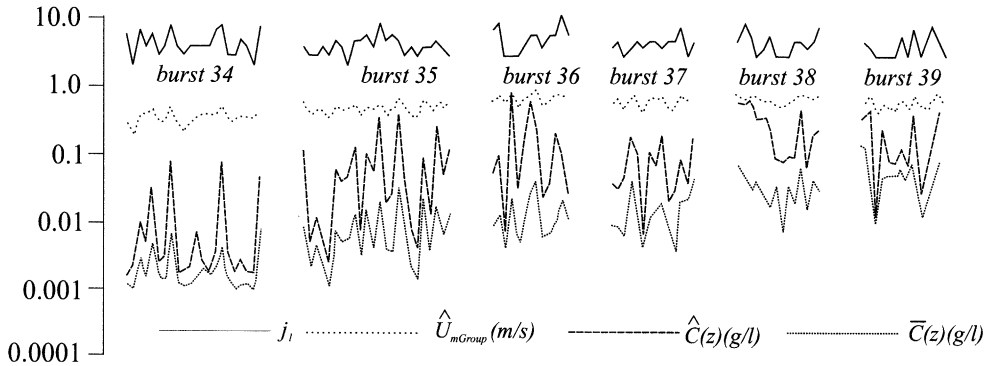

Fig. 4. Time-series plots showing j_1, $\hat{U}_{mGroup}$, $\hat{C}(z)$ and $\bar{C}(z)$ at $z = 2$ cm for bursts 34, 35, 36, 37, 38 and 39. Note: length of time axes differ between bursts.

through time. An increase in wave height during the present observational period results in an increase in $\hat{U}_{\mathrm{mGroup}}$ values through time from a value of approximately 36 cm/s during burst 34 to a maximum value of approximately 72 cm/s during burst 38, (Fig. 4). Similarly, Fig. 4 also shows an increase in $\bar{C}(z)$ and $\hat{C}(z)$ values measured at $z=$ 2 cm from 0.002 g/l and 0.0134 g/l, respectively, during burst 34 to 0.004 g/l and 0.308 g/l, respectively, during burst 38. The temporal increase in $\bar{C}(z)$ and $\hat{C}(z)$ values is primarily a response to a corresponding increase in wave height during this period. Apparent visual correlation between $\hat{C}(z)$ values, $\hat{U}_{\mathrm{mGroup}}$ values and j_1 values shown in Fig. 4 are considered below.

Histograms in Fig. 5a,b show the positively skewed frequency distributions for j_1 and j_2, (skewness 0.978 and 0.778, respectively). Fig. 5a shows that groups comprising three waves were

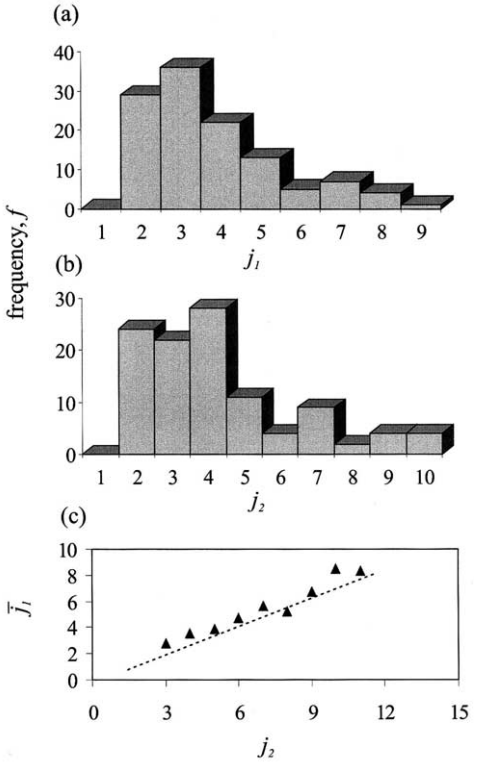

Fig. 5. (a) Frequency distribution for j_1. (b) Frequency distribution for j_2. (c) Linear relationship between $\bar{j}_1$ and j_2.

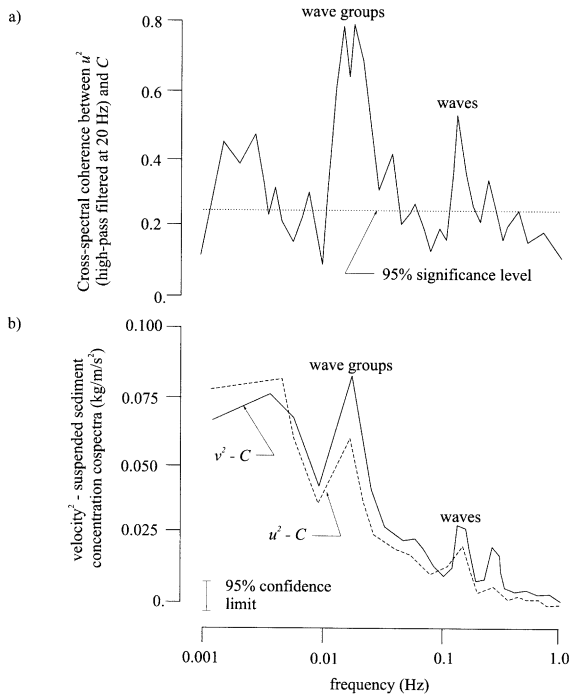

Fig. 6. (a) Cross-spectral coherence between u^2 (high-pass filtered at 20 Hz) and C (measured at $z=2$ cm) for burst 36. (b) u^2–C and v^2–C cospectra for burst 36 showing correlation between u and C and between v and C at wave group, wave and half wave frequencies C (C measured at $z=2$ cm).

the most frequent and that groups comprising more than six waves were uncommon. A linear relationship, significant at the 99% confidence level (product moment correlation coefficient, $R^2=0.942$), is found between j_2 and the average j_1 value, $\bar{j}_1$, associated with a given value of j_2, Fig. 5c. These data illustrate unequivocally, that groups containing many waves are proceeded by a long quiescent period, whereas groups containing smaller numbers of waves are proceeded by a shorter quiescent period.

Spectral analyses of hydrodynamic and sediment data were undertaken using a standard 4096 point fast Fourier transform (FFT with Hanning window and no overlap). Fig. 6a shows cross-spectral coherence between u^2 and C at $z=2$ cm for burst 36 (typical). Here, u^2 time-series have been high-pass filtered at 20 Hz to remove low frequency hydrodynamic forcing (Hanes, 1991). Fig. 6b shows the u^2–C and v^2–C cospectra for

burst 36 (C measured at $z = 2$ cm) obtained using the instantaneous (4 Hz) suspended sediment concentration time-series (C) and the instantaneous (smoothed to 4 Hz) horizontal flow components u and v. Similar cospectra are obtained for other burst records over the height range 1 cm $< z < 20$ cm during the storm period considered here.

The high coherence between u^2 and C illustrated in Fig. 6a shows clearly the effect of wave groups on resuspension of bed sediments. In addition, statistically significant correlation between u^2 and C and between v^2 and C at half wave (≈ 0.25 Hz), wave (≈ 0.125 Hz), wave group (≈ 0.01 Hz) and lower frequencies (approximately in the range 0.01 Hz to 0.003 Hz) are clearly demonstrated in Fig. 6b. It is considered that the strong linkage between fluid motions at approximately the wave group frequency and sediment resuspension shown in Fig. 6 demonstrates well the role of wave groups in enhancing local resuspension beyond a value accomplished by single waves alone. Similar results under shoaled wave, flat bed conditions in the nearshore region are presented by Hanes (1991).

Fig. 7 shows the amplitude of surface waves during three typical groups of waves measured during the experiment. Measured values of $\bar{C}_w(z)$ at $z = 2$ cm and computed values of $\hat{U}_{*wGroup}$ (Eq. 4) are also shown. Fig. 7 shows that $\bar{C}_w(z)$ values increase in response to increasing wave amplitude and demonstrate that the 'background' concentration of suspended sediments increases during the passage of a wave group. This result is not unexpected, and in common with finding reported by e.g. Hanes, 1991 and Lee et al., 1994, Fig. 7 simply shows that groups of larger than average waves result in enhanced resuspension of bottom sediments.

It has also been observed that the instantaneous C time-series show little evidence of an inter-wave period decrease in concentration in response to a reduction in $\hat{U}_{*wGroup}$ during a wave cycle. Given the relatively large in-situ grain settling velocity of the present sediments (O(5 cm/s), Fig. 1b), this observation by implication indicates that a succession of larger than average waves results in the generation of an enhanced vertical flux of momentum which supports a population of suspended material significantly larger than would be the case for single waves alone. Given the strong correlation between waves and resuspension events demonstrated above, it is not unreasonable to assume that the generation of additional turbulence, through separation and stretching of the wave boundary layer by the vortex ejection mechanism, is probably responsible for enhanced turbulent diffusion in the region above the bed considered here. It is likely that these mechanisms also enhance turbulent diffusion processes.

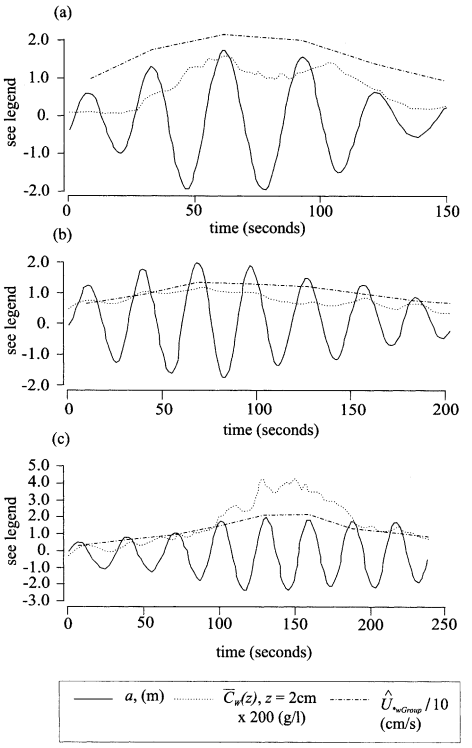

Fig. 7. Measured surface wave amplitude, a, measured wave-averaged suspended sediment concentration, $\bar{c}_w(z)$ at $z = 2$ cm and computed peak wave-only bed shear velocity, $\hat{U}_{*wGroup}$, for three wave groups containing: (a) 5 waves; (b) 7 waves; and (c) 8 waves.

The effect of wave groups in enhancing the local suspended sediment concentration beyond a value associated with a single wave with approximately the same amplitude is illustrated clearly by the computer-generated surface in Fig. 8. This figure includes all data from burst 34 to burst 39 and shows j_3, $\hat{U}_{mGroup}$ and $\bar{C}(z)$ for $z = 1$ cm on x, y and z axes, respectively. Consid-

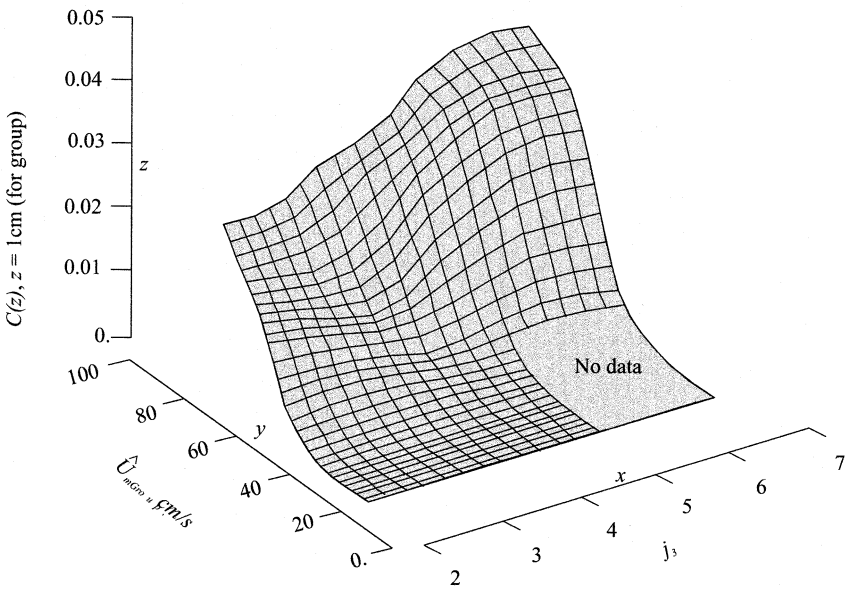

Fig. 8. Computer generated surface showing relationship between the wave group-averaged suspended sediment concentration, $\bar{C}(z)$, the peak group wave orbital velocity, $\hat{U}_{\mathrm{mGroup}}$, and j_3 values.

ering the y and z axes first, $\hat{C}(z)$ values are shown to increase approximately linearly with $\hat{U}_{\mathrm{mGroup}}$ from <0.001 g/l at $\hat{U}_{\mathrm{mG}}$ values ≈ 50 cm/s to 0.02 g/l at $\hat{U}_{\mathrm{mGroup}}$ values ≈ 100 cm/s. A threshold U_{m} value, U_{mT}, of ≈ 50 cm/s for suspension of the bed material implied by Fig. 8 is in accord with observed and predicted U_{mT} values for the present mixture of grain sizes shown in Fig. 1b, (Soulsby, 1997). Considering now the x axis in Fig. 8 it can be seen that for any given value of $\hat{U}_{\mathrm{mGroup}} > \approx 50$ cm/s, $\bar{C}(z)$ values increase with j_3 to attain a maximum value of approximately 0.05 g/l at the maximum $\hat{U}_{\mathrm{mGroup}}$ and j_3 values. This $\bar{C}(z)$ value is approximately three times larger that comparable $\bar{C}(z)$ values measured for groups of waves with the same $\hat{U}_{\mathrm{mGroup}}$ value and j_3 values of two. Thus, Fig. 8 shows clearly that wave groups enhance directly the resuspension of bed sediments.

Having now established that wave groups play an important role in the resuspension of the present sediments, it is useful now to examine means by which wave group effects can be incorporated into existing expressions for suspended sediment transport. Given that the present field data is site specific, it is not possible to formulate an expression with application across a broad range of sediment grain sizes or for situations where the hydrodynamic conditions may be significantly different. However, it is considered that the basic approach adopted here will have broader applications as more data becomes available.

Here, using multiple linear regression, we simply present a best fit empirical relationship between: a Rouse-type parameter, $(\hat{U}_{\mathrm{mGroup}}/w_{\mathrm{s}})$; j_3; and the normalised suspended sediment concentration at $z=1$ cm, $(\bar{C}(z)/\rho_{\mathrm{s}})$ in the form

$$\bar{C}(z) = \rho_{\mathrm{s}} G_1 \exp\left(j_3 + G_2 \frac{\hat{U}_{*\mathrm{mGroup}}}{w_{\mathrm{s}}} \right) \qquad (7)$$

where G_1 and G_2 are constants with values of -3.7 and 0.1 for the present data. Here, the $\bar{C}(z)$ value at 1 cm is chosen as it relates most closely to the familiar 'reference concentration' concept used in most expressions for vertical suspended sediment concentration profiles. In Fig. 9 $\bar{C}(z)$ values predicted by Eq. 7 are plotted against $\bar{C}(z)$ values measured at $z=1$ cm. The linear relationship between the predicted and the measured

values shown in Fig. 9 is statistically significant at the 95% confidence level ($R^2 = 0.89$). Correlation coefficient values > 0.8 are obtained for the relationship between observed and predicted $\bar{C}(z)$ values up to $z = 20$ cm. Values of $\bar{C}(z)$ predicted by Eq. 7 for $j_3 = 7$ are approximately a factor of three times larger than comparable $\bar{C}(z)$ values for $j_3 = 2$ (Fig. 8). Thus, for the present conditions, it is now possible to predict empirically, a near-bed concentration for suspended sediments which incorporates the effect of wave groups and spans a suspended sediment concentration range of three orders of magnitude (0.001–1.0 g/l). Further, it is considered likely that the non-dimensional form of Eq. 7 may make it more widely applicable for a range of grain sizes.

The present measurements also showed that groups of waves modify significantly the vertical suspended sediment concentration profile, *C*-profile. This effect is illustrated in Fig. 10 which shows typical *C*-profiles measured under groups containing 3, 5, 7 and 9 waves over the height range 1 cm $< z <$ 60 cm. For clarity, $\bar{C}(z)$ values are shown at intervals of 10 cm for $z > 10$ cm. In order to make comparisons between the selected *C*-profiles meaningful, the average wave group amplitude, $\bar{a}_G$, is approximately 1.5 m for each of *C*-profiles illustrated. Also shown in Fig. 10 are *C*-profiles predicted by a semi-empirical model derived by Williams et al. (1998). In the model, *C*-profiles are described by

$$\bar{C}(z) = \bar{C}(\gamma)\left(\frac{z+L}{a+L}\right)^{-\alpha} \tag{8}$$

where $\bar{C}(z)$ is the suspended sediment concentration at height z, $\bar{C}(\gamma)$ is the suspended sediment concentration at height γ, α is a Rouse-type parameter $= w_s/\kappa(\hat{U}_{*wcR} + \hat{U}_{*wG})$, κ is von Kármán's constant (0.4), $\bar{U}_{*wcR}$ is the time-averaged bed shear velocity in combined wave–current conditions for ripple-scale roughness, $\hat{U}_{*wG}$, is the peak wave shear velocity for grain-scale roughness, L is a turbulent length scale (Nielsen, 1992) $= \varepsilon_w/\kappa(\bar{U}_{*wcR} + \hat{U}_{*wG})$ and ε_w is the constant term consistent with the parameterisation of the vortex shedding-ejection mechanism in oscillatory flows over ripples. Here, values for $\bar{C}(\gamma)$ at $\gamma =$ 1 cm were calculated using Eq. 7, $\bar{U}_{*wcR}$, $\hat{U}_{*wG}$ and ε_w were calculated using the methods described by Williams et al. (1999) and values for α were obtained using a process of iteration to obtain the best fit to the observations (Williams et al., 1999).

Although further discussion of Eq. 8 is outside the scope of the present study, it is useful to compare *C*-profiles measured under groups of waves with *C*-profiles predicted using Eq. 8. For $\bar{C}$ val-

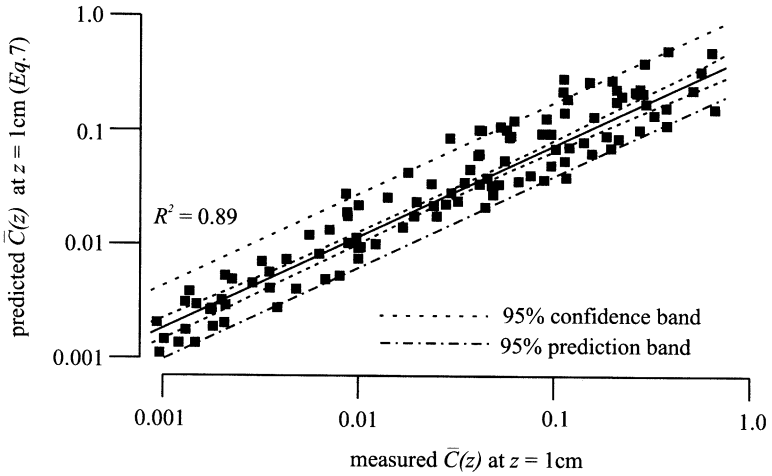

Fig. 9. Linear regression analysis of measured and predicted (Eq. 7) wave group-averaged suspended sediment concentration at $z = 1$ cm using data for all wave groups identified in burst 34 to burst 39.

ues spanning a range of 0.001–1.0 g/l, Fig. 10 shows clearly that irrespective of the height above the bed, the measured concentration of suspended sediment beneath groups of waves increases in response to an increase in j_1. This provides further evidence to support the view that wave groups enhance directly the vertical turbulent diffusion of sediments. Fig. 10 also shows that predicted C-profiles match closely the measured C-profiles and thus demonstrate that Eqs. 7 and 8 have a capacity to predict accurately the effect of wave groups on C-profiles.

With an increase in the vertical turbulent diffusion of sediments implied by results presented above, a corresponding increase in the grain size of suspended material might also be anticipated. Using measured values of $\bar{U}_{*\mathrm{wcR}}$ and $\hat{U}_{*\mathrm{wG}}$, and the values of α derived using Eq. 8, the in situ grain settling velocity under the influence of wave groups was calculated using

$$w_s = \alpha\kappa(\bar{U}_{*\mathrm{wcR}} + \hat{U}_{*\mathrm{wG}}) \quad (9)$$

Analysis of all wave groups from bursts 34 to 39 revealed an approximately linear relationship

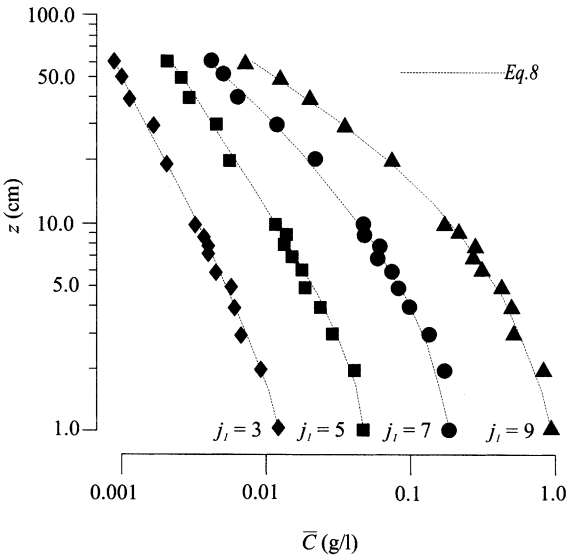

Fig. 10. Measured and predicted (Eqs. 7 and 8) wave group-averaged vertical suspended sediment concentration profiles for $j_1 = 3$, 5, 7 and 9.

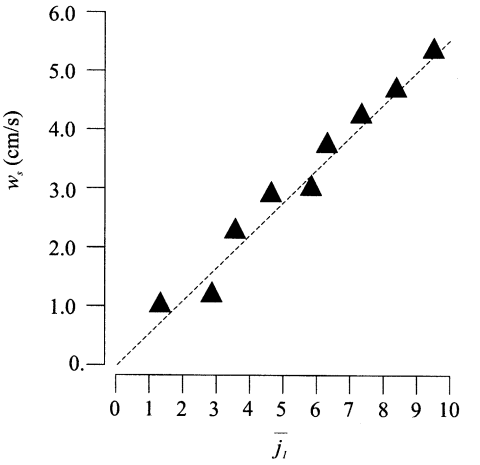

Fig. 11. Predicted grain settling velocity, w_s, under groups of $\bar{j}_1$ waves.

between $\bar{j}_1$ and w_s, Fig. 11. The w_s values imply that the median grain size in suspension for $\bar{j}_1 = 4$ was $\approx$210 μm ($w_s \approx 2$ cm/s), whilst for $\bar{j}_1 = 7$, the median grain size in suspension was $\approx$400 μm ($w_s \approx 4.0$ cm/s). These values are broadly in agreement with in situ particle size values of 180 μm and 350 μm for $\bar{j}_1 = 4$ and $\bar{j}_1 = 7$, respectively, measured by the ABS instruments. Whilst these data will not permit further examination of modifications to in situ settling velocity by wave and current-induced turbulence, the present results pertaining to grain size in suspension indicate further that wave groups affect the dynamic behaviour of sandy sediments and illustrate that wave group effects should be accounted for in methodologies to predict suspended sediment transport in the marine environment.

5. Conclusions

In situ observations of resuspension of medium/coarse sand by waves have been obtained in approximately orthogonal wave–current conditions during a moderate storm ($H_s = 2.1$–2.9 m) in 20 m water depth. A modified form of the Goda wave run-length analysis method has been used to identify and parameterise groups of waves. Frequency distributions for Goda parameters j_1 and j_2 were found to be positively skewed. A lin-

ear relationship has been found between j_2 and $\bar{j}_1$. Velocity-squared suspended sediment concentration cospectra show that resuspension events correlate strongly with half wave ($\approx$0.25 Hz), wave ($\approx$0.125 Hz), wave group ($\approx$0.01 Hz), and lower frequencies (0.01–0.003 Hz). $\bar{C}(z)$ values under groups of waves may be enhanced by a factor of three beyond that associated with single waves of comparable size. The 'background' concentration of suspended sediment has been observed to increases during the passage of a wave group. Since there was little evidence of inter-wave period grain settling it may be concluded that a series of larger than average waves increases the vertical flux of momentum. $\bar{C}(z)$ values have been found to increase in response to an increase in j_3.

A simple empirical expression has been derived to describe the relationship between ($\hat{U}_{\mathrm{mGroup}}$), j_3 and ($\bar{C}(z)/\rho_s$), and the in situ grain settling velocity has been shown to increase approximately linearly with $\bar{j}_1$. A capacity to predict the effect of wave groups on both the near-bed 'reference concentration' and on C-profiles has been demonstrated. Further investigations are required to fully validate the present observations. Present evidence indicates strongly that wave group effects must be considered when estimating the transport of sandy sediments in the marine environment. Wave groups are also likely to increase in significance with decreasing grain size.

6. Nomenclature

$\hat{A}$	peak semi-orbital wave excursion
$\bar{A}$	average semi-orbital wave excursion
C	instantaneous suspended sediment concentration
$\bar{C}_b$	burst-averaged suspended sediment concentration
$\hat{C}(z)$	peak suspended sediment concentration for a wave group at height z
$\bar{C}(z)$	average suspended sediment concentration for a wave group at height z
$\bar{C}(\gamma)$	average suspended sediment concentration for a wave group at height γ
$\bar{C}_w(z)$	average suspended sediment concentration beneath individual waves of height z
D	grain diameter
H	wave height
H_s	significant wave height
H_T	threshold wave height (Goda wave group analysis)
L	turbulent length scale (Nielsen, 1992)
R	product moment correlation coefficient
T_o	zero-crossing wave period
T_p	peak wave period
U	instantaneous horizontal flow component
$\bar{U}$	burst-averaged value of U
$\hat{U}_G$	peak horizontal flow component for the largest wave in a group
$\hat{U}_p$	measured instantaneous horizontal flow (port ECM head)
$\hat{U}_s$	measured instantaneous horizontal flow (starboard ECM head)
$\bar{U}_b$	burst-averaged wave orbital velocity
U_{mT}	threshold wave orbital velocity
$\hat{U}_{\mathrm{mGroup}}$	peak wave orbital velocity for a given wave group
$\hat{U}_{*\mathrm{wGroup}}$	peak wave-only bed shear velocity for a given wave group
$\bar{U}_{*\mathrm{wcR}}$	time-averaged bed shear velocity in combined wave–current conditions for ripple-scale roughness
$\hat{U}_{*\mathrm{wG}}$	peak wave-only bed shear velocity for grain-scale roughness
V	instantaneous horizontal flow component
$\bar{V}$	burst-averaged value of V
$\hat{V}_G$	peak horizontal flow component for the largest wave in a group
W	instantaneous vertical flow component
$\bar{a}_G$	average wave group amplitude
$\hat{a}_G$	peak wave group amplitude
d	water depth
f_w	wave friction factor (Jonsson, 1966)
g	acceleration due to gravity
h	bedform height
j_1, j_2, j_3	Goda wave group run-length parameters
$\bar{j}_1$	average of all j_1 values for a given j_2 value
k_s	physical bed roughness parameter
u	fluctuating part of the instantaneous U flow component comprising waves and turbulence
v	fluctuating part of the instantaneous V flow component comprising waves and turbulence
w_s	settling velocity for sediment grains
z	height above the sea bed
Ψ_s	dimensionless sediment mobility number
α	Rouse-type parameter
ε_w	constant parameterising the vortex shedding ejection mechanism in oscillatory flows over ripples
κ	von Kármán's constant (0.4)
λ	bedform wavelength
ρ	fluid density
ρ_s	measured sediment density
ω	radian wave frequency

Acknowledgements

The work was undertaken as part of the EU MAST 3 project 'Inlet Dynamics Initiative: Algarve' (INDIA). It was funded jointly by The Commission of the European Communities Directorate General for Science and Education, Research and Development under contract number MAS3-CT97-0106 and by the UK Natural Environment Research Council. Comments made by referees leading to improvements in the paper are gratefully acknowledged by the authors.

References

Bedford, K., Lee, J., 1994. Near-bottom sediment response to combined wave–current conditions, Mobile Bay, Gulf of Mexico. J. Geophys. Res. 99, 177.

Bishop, C.T., Donelan, M.A., 1987. Measuring waves with pressure transducers. Coast. Eng. 11, 309–328.

De Moor, G., Stolk, A., Chamley, H., Berne, S., Vincent, C., Houthuys, R., De Batist, M., 1993. Relationship between sea floor currents and sediment mobility in the southern North Sea. RESECUSED Final Report, European Commission MAST 1 Project, Contract Number MAST-0025-C, Commission of the European Communities Directorate General for Science and Education, pp. 195.

Goda, Y., 1985. Random Sea and Design of Maritime Structures. University of Tokyo Press.

Hanes, D.M., 1991. Suspension of sand due to wave groups. J. Geophys. Res. 78, 8911–8915.

Hanes, D.M., Huntley, D.A., 1986. Continuous measurements of suspended sand concentration in a wave dominated nearshore environment. Cont. Shelf Res. 6, 585–596.

Hannay, A., Williams, J.J., West, J.R., Coates, L.E., 1994. A field study of wave: current interactions over a rippled sandy bed. In: Belorgey, M., Rajaona, R.D., Sleath, J.A.F. (Eds.), EUROMECH 310: Sediment Transport Mechanisms in Coastal Environments and Rivers. World Scientific, River Edge, NJ, pp. 345–359.

Hedges, T.S., 1978. Some effects of currents on measurement and analysis of waves. Proc. Inst. Civ. Eng. Part 2 65, 685–692.

Humphery, J.D., Moores, S.P., 1994. STABLE II: An improved benthic lander for the study of turbulent wave–current–bed interactions and associated sediment transport. Electronic Engineering in Oceanography, IEE Conference Publication No. 394, pp. 170–174.

Jimenez, J.A., Arabi, A., Torres, R., Van Der Graff, J., Sanchez-Arcilla, A., 2000. On the predictability of suspended sediment pulses under non-breaking waves using groupiness' simple parameters. In: Edge, B.L. (Ed.), Proceedings Coastal Engineering 2000, Vol. 3, pp. 2850–2858.

Jonsson, I.G., 1966. Wave boundary-layers and friction factors. Proceedings of the 10th Conference on Coastal Engineering, Tokyo, Japan, 127–148.

Lee, J., O'Neil, S., Bedford, K., Van Evra, R., 1994. A bottom boundary layer sediment response to wave groups. Chapter 131, Coastal Engineering, 1994, ASCE, pp. 1827–1836.

List, J., 1991. Wave groupiness variations in the nearshore. Coast. Eng. 15, 475–496.

Longuet-Higgins, M., Stewart, R., 1964. Radiation stresses in water waves: a physical discussion, with applications. J. Fluid Mech. 13, 481–504.

Mansard, E.P.D., Sand, S.E., 1994. A comparative evaluation of wave grouping measures. Chapter 61, Coastal Engineering, 1994, ASCE, pp. 832–846.

Mase, H., 1989. Groupiness factor and wave height distribution. J. Waterways Port Coast. Ocean Eng. 115, 105–121.

Nielsen, P., 1981. Dynamics and geometry of wave generated ripples. J. Geophys. Res. 86, 6467–6472.

Nielsen, P., 1992. Coastal Bottom Boundary Layer and Sediment Transport. World Scientific, River Edge, NJ.

O'Connor, B.A., 1996. (Ed.), Handbook and Final Report: Circulation and Sediment Transport Around Banks (CSTAB), MAST 2 Project MAS-CT92–0024, Department of Civil Engineering, Report No, CE/05/96, University of Liverpool, Liverpool, UK, 2 Volumes, 633 pp.

Sato, S., 1992. Sand transport under grouping waves. In: Proceedings 23rd International Conference on Coastal Engineering, Paper 185.

Soulsby, R.L., 1997. Dynamics of marine sands. A manual for practical applications. HR Wallingford Report SR 466, 142 pp.

Soulsby, R.L., Goldberg, D.G., Stevenson, E.C., 1991. Norfolk Sand Banks. Analysis of STABLE data. HR Wallingford, Report Number EX 2345, 18 pp.

Southgate, H.N., Oliver, N., 1989. Efficient solution to the current-depth dispersion equation. HR Wallingford Report SR 181.

Thorne, P.D., Hardcastle, P.J., 1997. Acoustic measurements of suspended sediments in turbulent currents and comparison with in-situ samples. J. Acoust. Soc. Am. 101, 2603–2614.

Thorne, P.D., Hardcastle, P.J., Soulsby, R.L., 1993. Analysis of acoustic measurements of suspended sediments. J. Geophys. Res. 98, 899–910.

Williams, J.J., Rose, C.P., Thorne, P.D., O'Connor, B.A., Humphery, J.D., Hardcastle, P.J., Moores, S.P., Cooke, J.A., Wilson, D.J., 1999. Field observations and predictions of bed shear stresses and vertical suspended sediment concentration profiles in wave–current conditions. Cont. Shelf Res. 19, 507–536.

Williams, J.J., Macdonald, N.J., O'Connor, B.A., Pan, S., Player, R., 2000. Offshore sand bank dynamics. J. Mar. Syst. 24, 153–173.

Wylie, T., Taylor, K., Born, A.J., 1994. Design and calibration of the sediment tower. POL Internal Document No. 60, pp. 15 (unpublished manuscript).